Comparison of Eco-friendly Ti−M Bimetallic Coordination Catalysts and Commercial Monometallic Sb- or Ti-Based Catalysts for the Synthesis of Poly(ethylene-co-isosorbide terephthalate)

Shangdong Xie, Sitian Qian, Kaiyang Zhu, Lijiang Sun, Wenxing Chen, and Shichang Chen*

ACCESS | Metrics & More | Article Recommendations

ABSTRACT: Sustainable development greatly benefits from the effective synthesis of bio-based copolymers that are environmentally friendly. To enhance the polymerization reactivity for the production of poly(ethylene-co-isosorbide terephthalate) (PEIT), five highly active Ti−M (M = Mg, Zn, Al, Fe, and Cu) bimetallic coordination catalysts were designed. The catalytic activity of Ti−M bimetallic coordination catalysts and single Sb- or Ti-based catalysts was compared, and the effects of catalysts with a different type of coordination metal (Mg, Zn, Al, Fe, and Cu) on the thermodynamic and crystallization properties of copolyesters were explored. In polymerization, it was found that Ti−M bimetallic catalysts with 5 ppm (Ti) had higher catalytic activity than traditional antimony-based catalysts or Ti-based catalysts with 200 ppm (Sb) or 5 ppm (Ti). The Ti−Al coordination catalyst showed the best-improved reaction rate of isosorbide among the five transition metals used. Utilizing Ti−M bimetallic catalysts, a high-

quality PEIT was successfully synthesized with the highest number-average molecular weight of 2.82×10^4 g/mol and the narrowest molecular weight distribution index of 1.43. The glass-transition temperature of PEIT reached 88.3 °C, allowing the copolyesters to be used in applications requiring a higher T_g, like hot filling. The crystallization kinetics of copolyesters prepared by some Ti−M catalysts was faster than that of copolyesters prepared by conventional titanium catalysts.
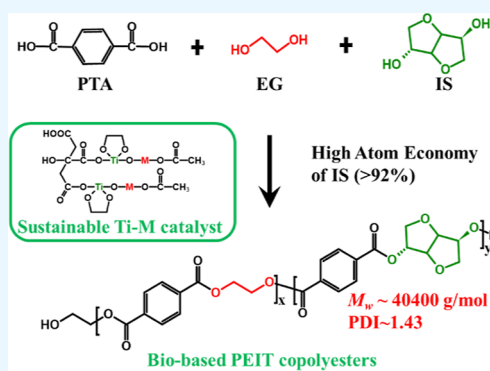
1. INTRODUCTION

Semicrystalline thermoplastic polyesters are in wide spread use in our daily life and engineering construction, ranging from bottles for carbonated soft drinks and water to fibers for apparels and string.[1−3] Although some polyesters, such as polytrimethylene terephthalate, polybutylene terephthalate (PBT), polyethylene naphthalate, and others, have been commercially successful, they cannot compete with polyethylene terephthalate (PET) in terms of cost-performance. PET has evolved into the most sought-after and most consumed material type in the fields of global textile, soft drink bottles, food packaging, and industrial fiber as a result of the simple availability of monomers and advanced production technology.[4,5] Synthetic bio-based polyesters have received a lot of attention in both research and application due to the limitation of petroleum resources. Due to PET's exceptional cost-effectiveness, researchers are constantly looking for ways to improve its performance through third monomer copolymerization, chemical grafting, and blending modification.[6−10]

Isosorbide is a diol with a cyclic structure that has been commercialized.[11−13] Numerous studies[14−20] have shown that isosorbide is a suitable building block for the design of bio-based materials. When copolymerizing PET,[21−23] PBT,[24,25] or other polyesters,[26−28] a small amount of isosorbide can significantly

lower the melting point and raise the T_g of the copolyester, and the T_g and T_m can be fine-tuned by adjusting the amounts of isosorbide added. Interestingly, Legrand et al.[29] prepared an amorphous and high glass-transition temperature (T_g) partially bio-based amorphous poly(tricyclodecanedimethylene-co-isosorbide terephthalate) (PTIT) using isosorbide as a third monomer; it was found that isosorbide enhanced the polycondensation kinetics and acted as a temporary chain linker, the polymerization kinetics improvement maximum was observed when the isosorbide content was around 9 mol %, and T_g linearly increased at 0.7 °C per mol % of isosorbide.

The low reactivity of the secondary hydroxyl group, which results in a polymer chain containing far less isosorbide than the feed ratio, is an unavoidable issue with the application of isosorbide in polymerization.[30] Bersot et al.[31] discovered that the catalytic system had higher catalytic efficiency at higher isosorbide content. Similarly, a bimetallic catalyst system based
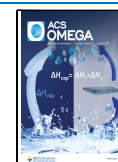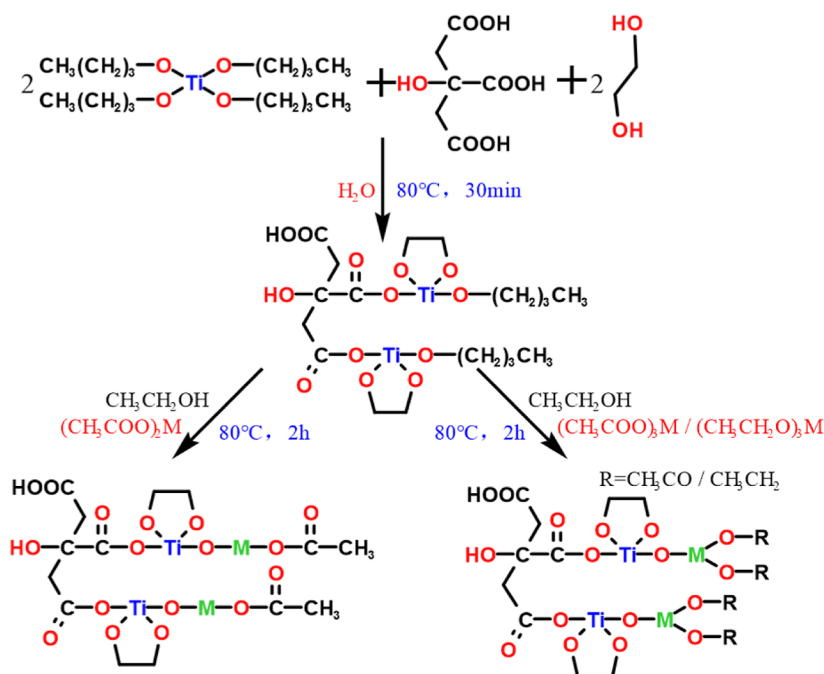
Scheme 1. Synthetic Pathways of Ti−M Bimetallic Coordination Catalysts

on two straightforward Sb, Ge, and Ti mixtures was used by Stanley et al.[32] There are not many reports on the use of bimetallic coordination catalysts based on titanium to increase isosorbide activity. Titanium-based catalysts are more environmentally friendly, do not lead to heavy metal pollution, and are nontoxic when compared with antimony-based catalysts. Actually, it has been well proven to promote reaction efficiency in the synthesis of certain polyesters.[33−37]

Herein, we concentrate on developing heavy metal-free Ti−M bimetallic coordination catalysts to compensate for the lack of reactivity of isosorbide in a polymer. An analysis of structural and thermal stability and catalytic activity of Ti−M catalysts has been carefully performed. The macromolecular chain structure and the typical important properties including the thermal processability and mechanical property differences of copolyesters prepared by Ti−M bimetallic coordination catalysis and conventional catalysts have been compared. The proposed Ti−M bimetallic catalysts are so active that isosorbide has higher polymerization efficiency to achieve high molecular weight and narrow molecular weight distribution. Additionally, a potential catalytic mechanism for the copolymerization of Ti−M bimetallic catalysts is proposed. It is anticipated that copolyesters would expand more wider application.

2. EXPERIMENTAL SECTION

2.1. Materials. Terephthalic acid (TPA), ethylene glycol (EG), isosorbide, phenol, magnesium acetate, zinc acetate, aluminum ethoxide, citric acid, and tetra-butyl *ortho*-titanate (TBOT) were purchased from Shanghai Aladdin Biochemical Technology Co., Ltd. (Shanghai, China). Antimony trioxide, 1,1,2,2-tetrachloroethane diantimony trioxide, antimony glycolate, hydroxydiacetyl iron, copper acetate, bis(2-hydroxyethyl) terephthalate (BHET), and chloroform were bought from Shanghai Macklin Biochemical Technology Co., Ltd. (Shanghai, China). All materials were analytical reagents and used without further purification. Nitrogen gases were obtained from Hangzhou Jingong Special Gas Co., Ltd. (Hangzhou, China).

2.2. Synthesis of Ti−M Bimetallic Coordination Catalysts. Ti−M bimetallic coordination catalysts were prepared by a similar route as described in a reported work.[38] Citric acid (25 mmol) was used as a ligand by reacting with tetrabutyl titanate (50 mmol) in water (100 mL), while heating to 80 °C, after which an amount of EG (50 mmol) was added dropwise to react for 30 min. The reacted solution was filtered with suction and dried at 60 °C for 12 h. The dried product was transferred into ethanol, and coordination metal (50 mmol) was added subsequently. The solution was heated until the ethanol boiled and reacted for 2 h, filtered, and washed with suction. After vacuum-drying for 12 h at 60 °C, Ti−M catalyst powders were obtained for further characterization and use (yield: 86%). The synthetic pathways of Ti−M catalysts as shown in Scheme 1 could reasonably be given on the basis of a successful Ti−Mg catalyst according to the reported literature.[38] The catalysts are labeled Ti−Mg, Ti−Zn, Ti−Al, Ti−Fe, and Ti−Cu according to the addition of the second metal in the subsequent description.

2.3. Synthesis of PEIT Copolyesters. TPA, EG, and isosorbide were added to a stainless steel stirred reactor [XSF-1.5(1.5L), Weihai Xingyu Chemical Machinery Co., Ltd., Weihai, China] with a ratio of acid (1.95 mol) to alcohol (2.73 mol) of 1:1.4 and IS/EG of 1:9. The catalyst [5 ppm of titanium and/or (2.5 ppm of Mg, 6.8 ppm of Zn, 2.81 ppm of Al, 5.8 ppm of Fe, and 6.6 ppm of Cu) or 200 ppm of antimony] was mixed with EG and added at the same time. Then, stirring was turned on, and the system was heated to 250 °C in 1 h for esterification reaction in a nitrogen environment. When the water yield reaches more than 90% of the theoretical value, the esterification is determined to be completed. Following the esterification stage, the pressure of the system was slowly lowered to carry out pre-polycondensation for 15 min. The system was then heated to 270 °C and evacuated to less than 100 Pa. When the power reached a certain value at a fixed rpm, it was judged that the polycondensation was completed, and the reaction products were discharged into the cooling water, drawn into a strip shape, and cut into a pellet using a pelletizer. The

prepared polyester chips were dried in a vacuum oven at 80 °C for 24 h to remove moisture. The PEIT copolyesters prepared by different catalysts, Sb$_2$O$_3$, Sb$_2$(OC$_2$H$_4$O)$_3$, TBOT, Ti−Mg, Ti−Zn, Ti−Al, Ti−Fe, and Ti−Cu, were named as PEIT 1 to PEIT 8 sequentially.

2.4. Characterization. Before all analyses, the catalysts were dried at 60 °C for 12 h, and the PEIT chips were dried at 80 °C for 24 h in a vacuum oven. Fourier transform infrared (FT-IR) spectroscopy of Ti−M catalysts and PEIT was performed on a Nicolet 5700 FT-IR (Thermo Electron, Massachusetts, USA). A small number of different samples were mixed with KBr separately at room temperature and pressed for the infrared test. X-ray photoelectron spectroscopy (XPS) was performed on a K-Alpha spectrometer (Thermo Fisher Scientific, Massachusetts, USA). The nuclear magnetic resonance (NMR) analyses used the AVANCE AV400 MHz NMR spectrometer (Bruker, Karlsruhe, Germany). The polymer was dissolved in trifluoroacetic acid before analysis and analyzed at 25 °C for NMR.

The intrinsic viscosity (IV) analyses of PEIT were performed using a Visco 070 Ubbelohde viscometer (Julabo, Seelbach, Germany). PEIT was dissolved in a mixed solvent of phenol and tetrachloroethane (50/50 wt/wt) to formulate a concentration of about 0.5 g·dL^{-1}, and the intrinsic viscosity of PEIT was measured in a constant-temperature water tank at 25 °C. The tensile stress analyses used the 34TM-30 universal testing machine (Instron, Boston, USA).

The differential scanning calorimetry (DSC) analyses used the DSC3 STARe system (Mettler Toledo, Zurich, Switzerland). All experiments of catalysts and PEIT were performed under a 40 mL/min nitrogen atmosphere. Before analysis, BHET and the catalyst were mixed uniformly with a mole ratio of Ti to BHET of 1:50 to analyze the catalyst activity. For the thermal property testing of catalysts, the samples were heated at a constant rate of 10 °C/min from 25 to 280 °C. For PEIT, the samples were heated at a constant rate of 10 °C/min from 25 to 280 °C and kept at 280 °C for 3 min to remove the thermal history of the samples; then, the sample were quenched to 0 °C at a constant rate of 50 °C/min and kept at 0 °C for 3 min; the temperature was raised from 0 to 280 °C at a constant rate of 10 °C/min to obtain a temperature rise curve and then kept for 3 min; finally, the temperature was reduced to 0 °C at a constant rate of 10 °C/min to obtain a temperature drop curve. Before the isothermal crystallization measurements, the copolyester was heated from 25 to 280 °C at a rate of 20 °C/min and held at 280 °C for 5 min to eliminate thermal history. Then, the temperature was lowered to the target temperature at a rate of 50 °C/min for isothermal crystallization. The thermogravimetric (TGA) analyses used the TGA/DSC1 STARe system (Mettler Toledo, Zurich, Switzerland). Under a nitrogen flow of 40 mL/min, the samples were heated at a constant rate of 10 °C/min from 25 to 800 °C to obtain the TGA curve.

The molecular weight and molecular weight distribution information was determined by a multidetector size exclusion chromatography system obtained by advanced polymer chromatography (APC; Waters; Milford, Massachusetts) coupled with multi-angle laser light scattering (MALLS DAWN HELEOS II; Wyatt; Santa Barbara, California, USA) and a differential refractometer (Optilab T-rEX; Wyatt; Santa Barbara, California, USA).[39] The eluent at 25 °C used was hexafluoroisopropanol (HFIP). The samples were dissolved in HFIP to prepare a 2 mg/mL solution, and 50 μL was injected per analysis.

Tensile testing was performed on an Instron 34TM-30 using dumbbell-shaped specimens of 2 mm thickness and 4 mm width at strain rates of 10 mm min^{-1}; the specimens were prepared by a micro-injection molding machine (SZS-20, Ruiming, Wuhan, China).

3. RESULTS AND DISCUSSION

**3.1. Structural and Thermal Stability Analysis of Ti−M Catalysts.** The chemical structure of the catalysts was
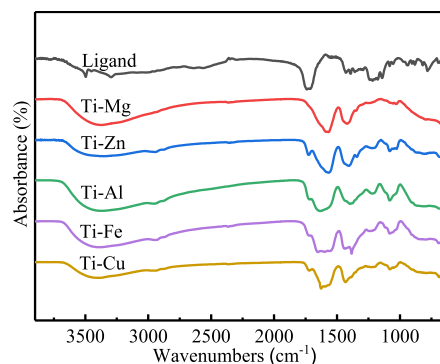

Figure 1. FT-IR spectra of the ligand and catalysts.

determined by FT-IR and XPS.[38,40,41] Figure 1 shows the infrared spectra of the ligand and different bimetallic coordination catalysts. The characteristic absorption peaks of the ligand were the stretching vibration peak of the hydroxyl group (ν −OH) in the carboxyl group (−COOH) at 3497 cm^{-1}, the strong carbonyl (ν C═O) stretching vibration peak at 1720−1730 cm^{-1}, and the flexural vibration peak of the hydroxyl group (δ −OH) at 850−950 cm^{-1}, which was due to the presence of three carboxyl groups and one hydroxyl group in citric acid. But for the five Ti−M catalysts, the infrared spectra have almost the same changes. The strong peak at 3497 cm^{-1} disappeared, which indicated that the carboxyl group in the ligand has undergone a chemical reaction, causing the disappearance of two of the three carboxyl groups.[42] The strong carbonyl stretching vibration peak in the ligand at 1730 cm^{-1} almost disappeared and completely disappeared in the Ti−Mg catalyst, which showed that all the three carboxyl groups in the Ti−Mg catalyst were coordinated, but in the other four catalysts, part of the carboxyl group was coordinated with metal ions. At the same time, the COO− asymmetric stretching vibration peak at 1570 cm^{-1} and the COO− symmetric stretching vibration peak around 1410 cm^{-1} appeared, which also indicated that the ligand and the metal ion were coordinated.[42]

The change of atomic valence or the combination of atoms with different electronegativities would cause the chemical environment of the atoms to change, which leads to chemical shifts of the peaks in the X-ray photoelectron spectrum. The XPS spectra of Ti−Al and the ligand are shown in Figure 2. By comparing Figure 2a,b, it can be seen that the ratio of the O 1s peak intensity to the C 1s peak intensity of the Ti−Al catalyst is significantly lower than that of the ligand, indicating that the ligand has reacted and lost part of oxygen atoms. Figure 2c shows the C 1s electron spectra of the Ti−Al catalyst and ligand. The peak with a binding energy of 284.6 eV mainly comes from the aliphatic carbon atoms (C−C) in the compound, and the peak at 286.5 eV comes from the carbon atom connected to the hydroxyl group (C−OH). Since the ligand has three carboxyl groups, the peak of the carboxyl carbon atom (CO−OH) of the
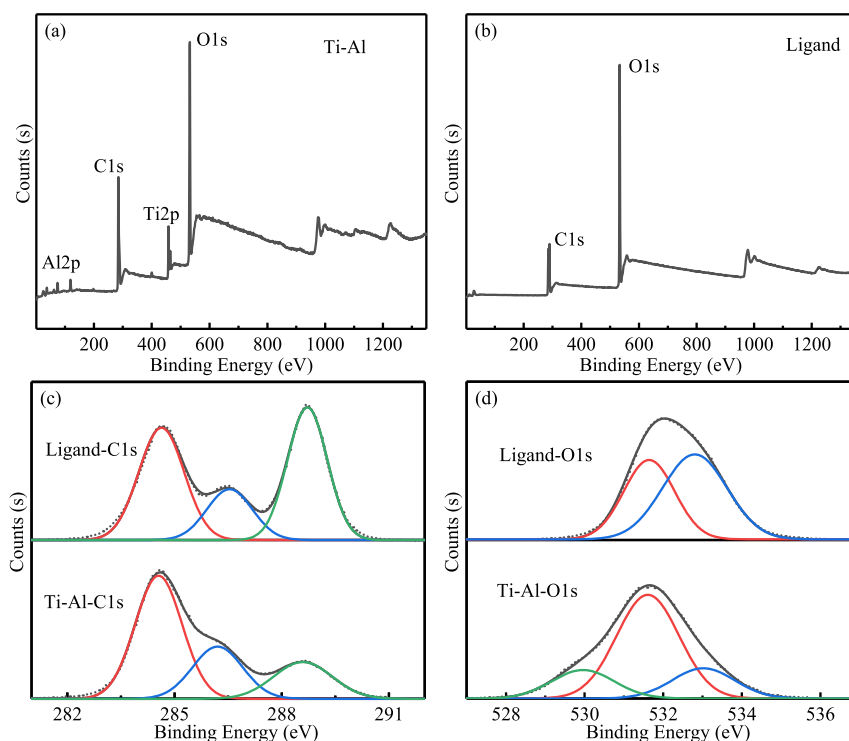
Figure 2. (a) XPS image of the Ti−Al catalyst. (b) XPS image of the ligand. (c) C 1s electron spectra of the ligand and Ti−Al catalyst. (d) O 1s electron spectra of the ligand and Ti−Al catalyst.
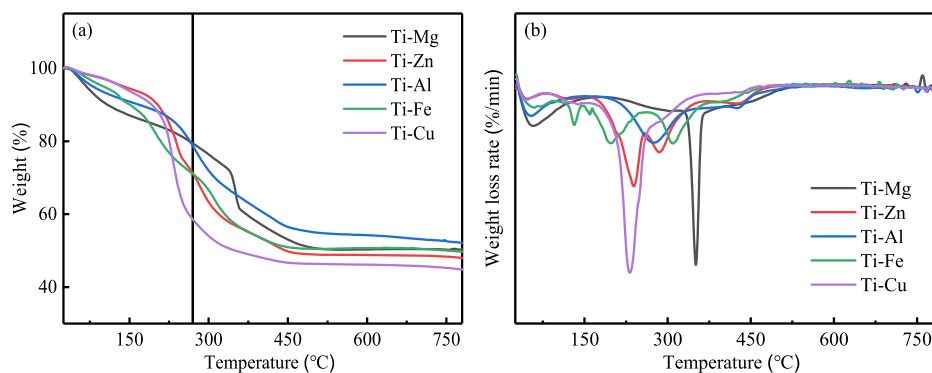

Figure 3. (a) TGA curves of different bimetallic catalysts. (b) DTG curves of different bimetallic catalysts.

ligand at 288.7 eV is very strong, which is greatly weakened in the Ti−Al catalyst. It shows that part of the carboxyl group in the ligand has reacted, which was consistent with the conclusion obtained by FT-IR. Figure 2d shows the O 1s electron spectra of the Ti−Al catalyst and ligand. In the ligand, the oxygen atom was mainly in two chemical environments: the carbonyl group and the hydroxyl group in the carboxyl group, and the binding energy was 531.6 and 532.8 eV, respectively. A peak with a binding energy of 529.9 eV appears in the spectrum of the Ti−Al catalyst. This was due to the combination of oxygen atoms and metal ions, which increases the density of the outer electron cloud of oxygen atoms and reduces the binding energy.[43] In addition, because the carboxyl group in the ligand was not completely coordinated with the metal, some of the oxygen atoms still existed in the form of carboxyl groups.

To ensure the thermal stability of the catalyst, a TGA test was conducted to make it clear that the catalysts could exist stably at the polymerization temperature and maintain high catalytic activity. The TGA and DTG curves of five bimetallic

coordination catalysts are shown in Figure 3. According to Figure 3a, the thermal decomposition of the five catalysts can be roughly divided into three stages: 25−170 °C, 170−270 °C, and above 270 °C. At 25−170 °C, the mass loss is mainly due to the evaporation of water in the catalyst and the removal of bound water. After the temperature rises to 170−270 °C, the uncoordinated small molecules in the catalyst begin to degrade. This degradation was more obvious for Ti−Cu, Ti−Zn, and Ti−Fe catalysts, indicating that these three catalysts may contain more small molecules. At 270 °C, the mass residues of Ti−Mg and Ti−Al catalysts were 80%, the mass residues of Ti−Zn and Ti−Fe catalysts were about 70%, and the mass residue of the Ti−Cu catalyst was only less than 60%. This shows that the Ti−Cu catalyst is not as stable as the other four catalysts at polycondensation temperature. Above 270 °C, what happens was decomposition and carbonization of the catalyst. Compared with Figure 3b, it can be seen that the thermal stability of Ti−Mg and Ti−Al catalysts is slightly higher than that of the other three catalysts, and the obvious degradation temperature of the Ti−
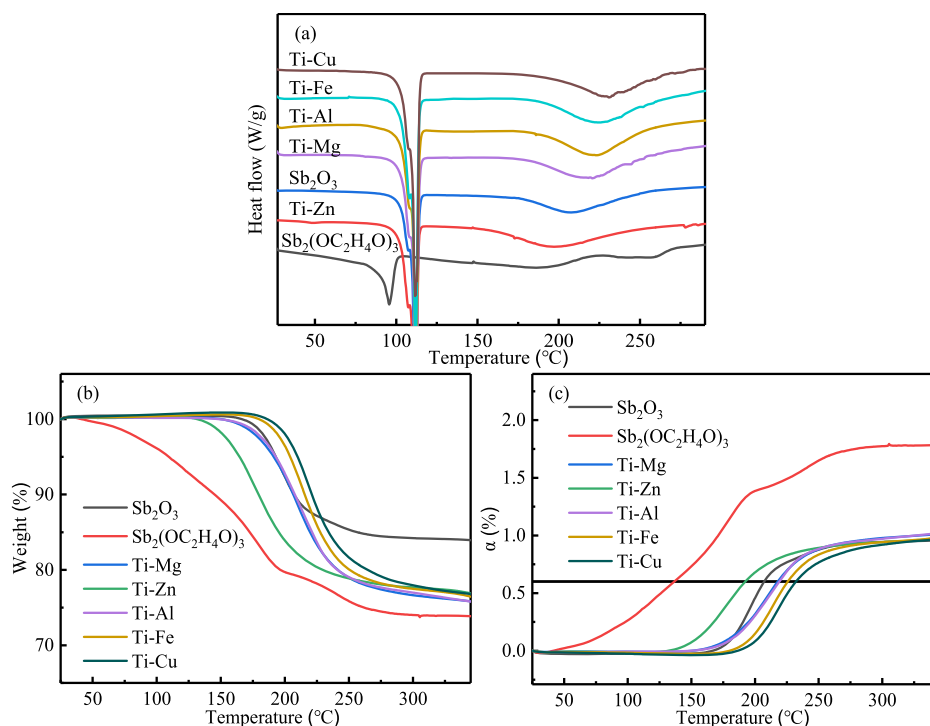
Figure 4. (a) DSC curve of BHET polycondensation over different catalysts. (b) TGA curve of BHET polycondensation over different catalysts. (c) Conversion curve of BHET polycondensation over different catalysts.
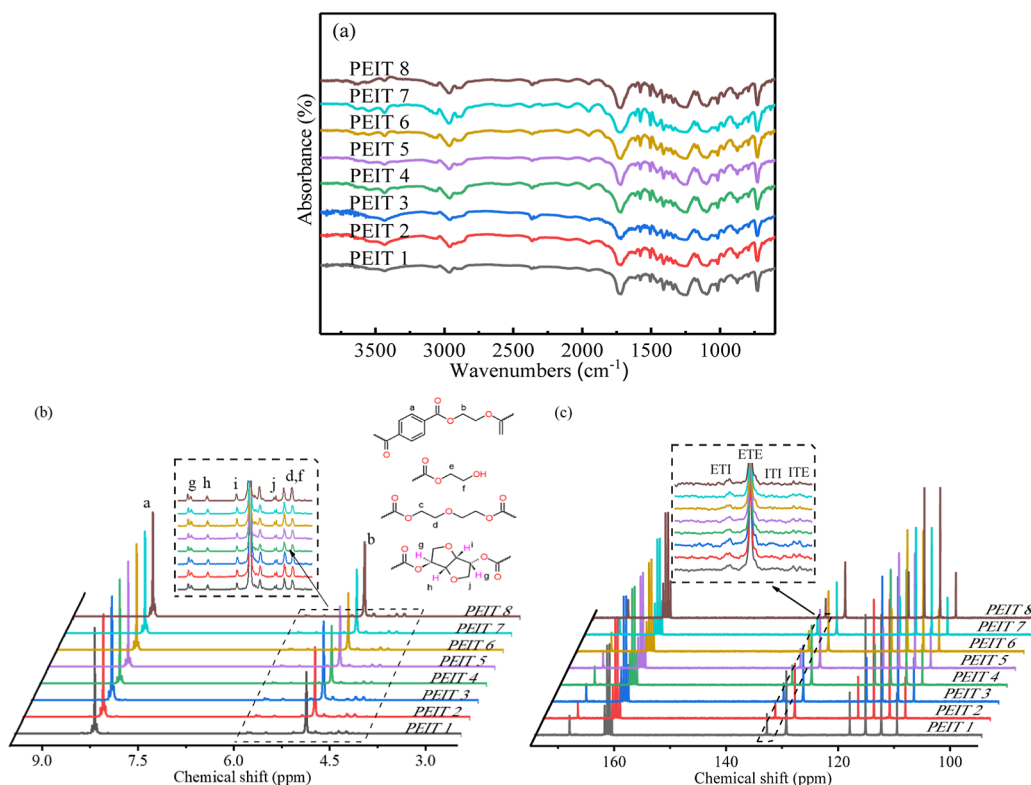
Figure 5. (a) Infrared spectra of copolyesters. (b) ^{1}H NMR spectra of copolyesters. (c) ^{13}C NMR spectra of copolyesters.

Mg catalyst is about 350 °C. Therefore, several catalysts are thermally stable enough to not decompose under polymerization conditions.

3.2. Catalytic Activity Analysis of Ti−M Catalysts. To get an understanding of the activity of the five bimetallic

coordination catalysts, a combination of DSC and TG was used for testing. Figure 4a shows the heating curve in DSC after mixing the catalysts and BHET. The catalytic activity of the catalysts for BHET can be determined by the temperatures of the endothermic peak after the melting peak of BHET.[44] It can

Table 1. Sequence Structure Parameters of Copolyesters

copolyesters	IS/EG	n_{ET}	n_{IT}
PEIT 1	7.82/92.18	13.17	1.60
PEIT 2	8.55/91.45	11.84	1.24
PEIT 3	8.16/91.84	13.52	1.47
PEIT 4	6.90/93.10	14.05	1.35
PEIT 5	7.21/92.79	13.90	1.41
PEIT 6	9.23/90.76	14.65	1.55
PEIT 7	7.75/92.25	13.24	1.15
PEIT 8	7.42/92.58	14.31	1.29

be seen from Figure 4a that the activity order of the seven catalysts is Ti−Zn > Sb$_2$O$_3$>Ti−Mg > Ti−Al > Ti−Fe > Ti−Cu > Sb$_2$(OC$_2$H$_4$O)$_3$. The content of antimony-based catalysts used was usually 40 times that of titanium-based catalysts, which led to the mass ratio of antimony-based catalysts to BHET reaching 2:5 and 2:3 in the activity test. The mixing of Sb$_2$(OC$_2$H$_4$O)$_3$ and BHET causes the melting point of BHET to drop, and the curve is inclined due to the change of heat flow generated by the catalyst itself. A broad endothermic peak can be seen around 250 °C, but the specific temperature cannot be determined. The TGA curves of the mixtures of catalysts and BHET are shown in Figure 4b. The EG produced by the polymerization reaction of BHET will continue to be taken away by nitrogen as the temperature rises, which causes the mass to continue to decline. Since EG was taken away by nitrogen, the reaction can be regarded as an irreversible reaction, so the progress of the polymerization reaction can be judged by mass loss. Introducing the conversion rate α, in this reaction, the theoretical maximum mass loss of BHET after the poly-condensation reaction is 24.4%, so the relationship between the conversion rate α and the quality is

$$\alpha = \frac{m_0 - m_t}{m_0 \times 24.4\%} \tag{1}$$

where m_0 is the initial mass of BHET and m_t is the remaining mass of BHET at time t.

Since the molar ratio of antimony atoms to BHET reached 40:50 when using antimony-based catalysts, the catalyst mass could not be ignored, so the BHET ratio γ was brought in to calculate the true mass of BHET in the test substance.

$$\gamma = \frac{m_b}{m_b + m_c} \tag{2}$$

$$m_0 = m \times \gamma \tag{3}$$

where γ is the proportion of BHET in the mixture, m_b is the added mass of BHET in the mixture, m_c is the added mass of the catalyst in the mixture, and m is the mass of the mixture weighed for testing.

The relationship curves between α and temperature obtained according to the calculation formula are shown in Figure 4c. $T_{\alpha=0.6}$ is taken as the basis for judging the catalyst activity. The mixture of EG antimony and BHET, due to the degradation of EG antimony itself, leads to a significant decrease in the mass of the early stage, and its activity cannot be judged. The catalyst activity order is Ti−Zn > Sb$_2$O$_3$ >Ti−Mg > Ti−Al > Ti−Fe > Ti−Cu > Sb$_2$(OC$_2$H$_4$O)$_3$, which was consistent with the results obtained by DSC.

3.3. Effect of Catalysts on the Structure of Copolyesters. The wavenumber of the infrared absorption peak of the same functional group is not fixed, and its position is affected by various factors such as the electronic effect, hydrogen bonding, vibration coupling, spatial effect, etc.[45,46] Figure 5a shows the infrared spectra of PEIT prepared using the Ti−M catalyst. It can be seen that the hydroxyl (−OH) stretching vibration peak is located at 3433 cm^{-1}. The methylene (−CH$_2$−) stretching vibration peak can be observed at 2964 cm^{-1}, and the carbonyl (C═O) stretching vibration peak in the PEIT main chain is at 1722 cm^{-1}. The ester groups (−COO−) formed by EG, isosorbide, and TPA correspond to the peaks at 1105 and 1243 cm^{-1}, and it can be judged that an esterification reaction has occurred in the system.

Figure 5b shows the ^{1}H-NMR spectra of the PEIT copolyester prepared by different catalysts. The reactivity of isosorbide is much weaker than that of EG, and the ratio of different monomer units in the polymer can be calculated from the hydrogen nuclear magnetic resonance spectrum. The difference in the catalytic activity of different catalysts for isosorbide can be expressed by the actual ratio β of isosorbide in the polymer chain, and the specific values are shown in Table 1. The calculation formula for isosorbide content is as follows

$$\beta = \frac{I_g + I_h + I_i + I_j}{2I_b} \tag{4}$$

The calculation results show that the Ti−Al catalyst has higher catalytic activity for isosorbide, and the content of isosorbide in PEIT prepared by it was higher than 9%.

The average sequence length of the copolymer and the activity R can be calculated by calculating the carbon NMR spectrum of the copolymer to characterize the structure of the copolyester. The four different segment sequences in the PEIT copolyester correspond to the four peaks of k (ETI), l (ETE), m (ITI), and n (ITE) in Figure 5c, respectively.[47] The specific values of average sequence length and activity are shown in Table 1, and the calculation formula is as follows

$$n_{ET} = \frac{S_{ETE} + (S_{ITE} + S_{ETI})/2}{(S_{ITE} + S_{ETI})/2} \tag{5}$$

Table 2. Molecular Weight and Molecular Weight Distribution Information of PEIT

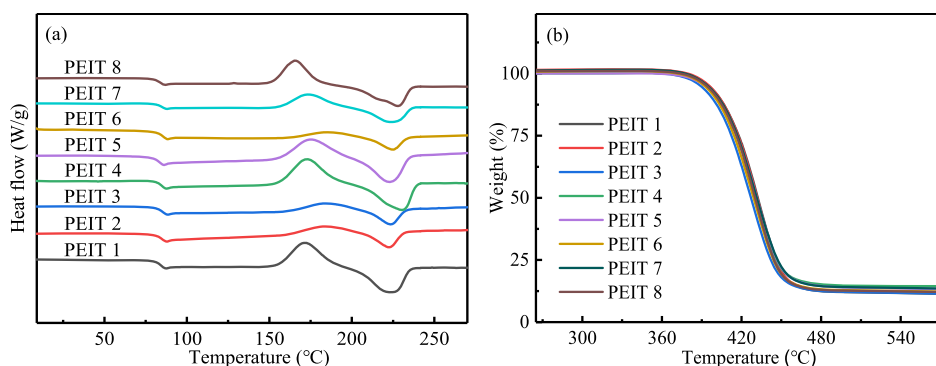| copolyesters	dosage of Sb/Ti(Ti−M) (ppm)	reaction time (h)	IV (dL/g)	M_n (10^4 g/mol)	M_w (10^4 g/mol)	PDI
PEIT 1	200	4.9	0.61	2.18	3.63	1.67
PEIT 2	200	4.7	0.64	2.54	3.88	1.53
PEIT 3	5	4.3	0.63	2.51	3.80	1.53
PEIT 4	5−2.5	4.0	0.64	2.74	4.01	1.46
PEIT 5	5−6.8	4.1	0.65	2.61	3.91	1.50
PEIT 6	5−2.81	4.3	0.65	2.79	4.21	1.51
PEIT 7	5−5.8	4.4	0.65	2.65	4.23	1.60
PEIT 8	5−6.6	4.4	0.64	2.82	4.04	1.43

Figure 6. (a) DSC heating curves of copolyesters. (b) TGA curves of copolyesters.

Table 3. Thermal Property Parameters of Copolyesters

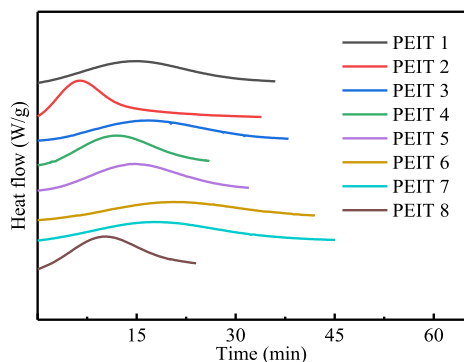| copolyesters	T_g (°C)	T_c (°C)	T_m (°C)	$T_{5\%}$ (°C)	$T_{d,max}$ (°C)
PEIT 1	87.3	171.3	224.3	395.3	433.7
PEIT 2	87.7	183.3	222.3	395.7	433.0
PEIT 3	88.0	184.3	223.7	389.3	427.0
PEIT 4	87.7	173.0	230.3	393.3	430.7
PEIT 5	86.0	175.3	223.0	392.3	431.7
PEIT 6	88.3	186.0	224.7	392.0	431.0
PEIT 7	87.7	173.7	223.7	394.7	429.7
PEIT 8	86.7	165.7	227.7	393.7	429.3

Figure 7. DSC isothermal crystallization curves of copolyesters at 170 °C.
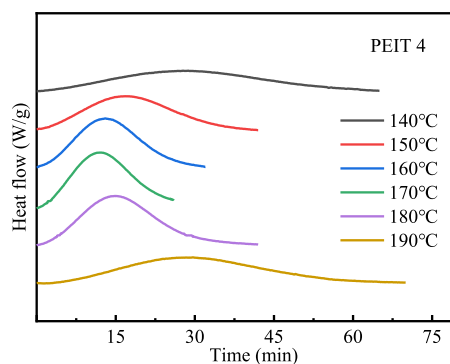

Figure 8. DSC isothermal crystallization curves of the PEIT 4 catalyst at different temperatures.

$$n_{IT} = \frac{S_{ITI} + (S_{ITE} + S_{ETI})/2}{(S_{ITE} + S_{ETI})/2} \tag{6}$$

$$R = \frac{1}{n_{ET}} + \frac{1}{n_{IT}} \tag{7}$$

The values of R of PEIT 2 and PEIT 7 were closer to 1, indicating that the PEIT copolyester prepared by these two catalysts was closer to random copolymerization.

The molecular weight and molecular weight distribution information of PEIT copolyesters obtained from the Ubbelohde viscometer and APC is presented in Table 2; the catalyst dosage is calculated in terms of the content of antimony atom or titanium atom in catalysts. According to the reaction time, it can be seen that the catalytic activity of 5 ppm Ti-based catalysts for PEIT is much greater than that of 200 ppm Sb-based catalysts, and the reaction time was shortened by up to 0.9 h compared with antimony trioxide. The IV of PEIT is between 0.61 and 0.65 dL/g; no significant difference can be noted among several PEITs by using Ti−M catalysts. From the number-average and weight-average molecular weight data, it can be seen that the number-average molecular weight of PEIT 4, PEIT 6, and PEIT 8 is higher than that of those prepared by other catalysts. This may be because although the Ti atom and the ligand were coordinated to cause its catalytic activity to decrease, the added second metal (Mg, Al, and Cu) itself also has better catalytic activity for the polyester. This part of the activity not only makes up for the part of the activity that was inhibited by Ti but even makes the catalyst show a higher activity as a whole. In addition, because the activity of the catalyst increases, all the polymer chains grow faster, and the molecular weight distribution of PEIT is narrower. Consistent with the catalyst activity test, the polymerization time of PEIT 5 was only 4.1 h, but its thermal stability was slightly lower than that of PEIT 4, and some of the weakly bound coordination bonds might be broken, making the polymerization effect lower than that of the Ti−Mg catalyst.

3.4. Effect of Catalysts on the Thermal Properties of Copolyesters. DSC and TGA were performed to investigate the difference in the thermal properties for copolyesters with different catalysts. Figure 6a presents the DSC curves of PEIT during second heating. It appears that all curves display an endothermic event and an exothermic event taking place over a varying period depending on the catalysts used. The values of glass-transition temperature (T_g), crystallization temperature (T_c), and melting temperature (T_m) are listed in Table 3. After adding 10% isosorbide, the T_g of the polyesters shifts toward higher values (above 85 °C). In addition, the T_g values of PEIT 3 and PEIT 6 are slightly higher, which may be related to the more isosorbide units in the polymer chain, as shown in the result of ^{1}H NMR. PEIT 6 has the highest cold crystallization temperature, and its crystallization peak is also the broadest.
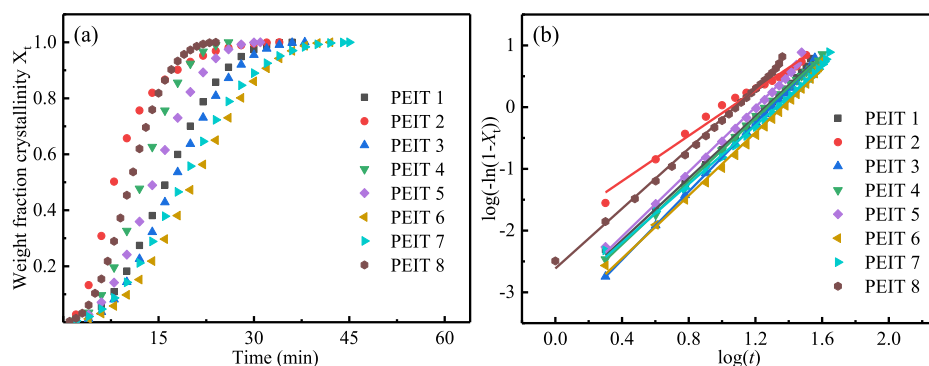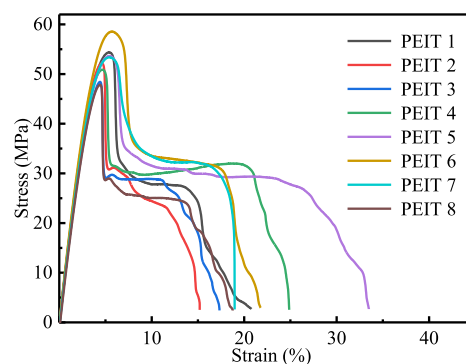
Figure 9. (a) Crystallinity X_t versus isothermal crystallization time t of copolyesters at 170 °C. (b) Log($-\ln(1 - X_t)$) versus log(t) of copolyesters at 170 °C.

Table 4. Isothermal Crystallization Kinetic Parameters of Copolyesters

catalyst	T (°C)	$t_{1/2}$ (min)	K (10^{-4} min^{-1})	n
PEIT 1	150	22.58	2.30	2.57
	160	14.58	8.83	2.49
	170	15.75	6.94	2.51
	180	18.38	3.50	2.61
PEIT 2	150	19.75	46.60	1.68
	160	13.43	78.00	1.73
	170	9.25	116.00	1.84
	180	11.70	54.00	1.97
PEIT 3	150	22.08	3.31	2.47
	160	18.05	2.84	2.70
	170	17.26	2.62	2.77
	180	22.33	3.73	2.42
PEIT 4	150	17.78	3.89	2.60
	160	13.67	7.19	2.63
	170	12.16	9.89	2.62
	180	16.24	5.66	2.55
PEIT 5	150	21.83	2.62	2.56
	160	15.34	10.5	2.38
	170	13.78	7.16	2.62
	180	21.63	1.68	2.71
PEIT 6	150	23.27	1.04	2.80
	160	20.06	1.87	2.74
	170	19.91	3.36	2.55
	180	25.27	1.10	2.71
PEIT 7	150	27.05	4.71	2.21
	160	21.43	2.25	2.62
	170	18.15	7.17	2.37
	180	22.95	2.23	2.57
PEIT 8	150	12.21	26.9	2.22
	160	10.50	19.6	2.50
	170	10.28	24.3	2.43
	180	16.48	5.95	2.52

Figure 10. Mechanical property curves of copolyesters prepared by different catalysts.

polymer chain, PEIT 4 has higher crystallinity, and the melting temperature is slightly higher than that of other samples.

The thermal stability of polymers is often judged by the TGA curve. As shown in Table 3 and Figure 6b, all samples have similar thermal decomposition temperatures. However, the maximum decomposition rate and the maximum decomposition rate temperature ($T_{d,max}$) of PEIT prepared with antimony-based catalysts were significantly higher than those of PEIT prepared with titanium-based catalysts. This is because titanium-based catalysts not only have strong catalytic activity for polycondensation reaction but also have strong catalytic activity for thermal degradation and thermo-oxidative degradation of polymers, which will result in lower thermal degradation temperature to a certain extent.[36]

3.5. Isothermal Crystallization Kinetics of PEIT. In order to provide a deeper study of the effect of catalysts on the crystallization properties of copolyesters, the crystallization kinetics of PEIT prepared by different catalysts were investigated. Figure 7 presents the isothermal crystallization DSC curves of PEIT copolyesters prepared by different catalysts at 170 °C. It appears in this figure that the tape of the catalyst used in the polymerization process has a great influence on the crystallinity of the copolyester. PEIT 4 and PEIT 8 have faster crystallization rates among several copolyesters, and PEIT 2 apparently has a faster crystallization rate in the early stage, but the crystallization rate in the later stage obviously reduces, which leads to the prolongation of its complete crystallization time; it is related to its wider molecular weight distribution. Crystallization is completed in a short time, but the remaining larger molecular weight fraction can only crystallize at a slower rate.

The cold crystallization temperature has a positive correlation with its peak width, that is to say, the higher the cold crystallization temperature, the wider the crystallization peak. This is due to the uneven distribution of isosorbide in PEIT, which makes the crystallization performance of the part containing more isosorbide relatively worse; thus, it requires a longer crystallization time, thereby broadening the cold crystallization peak. Almost all samples have similar melting temperatures. Due to the lower content of isosorbide in the

Scheme 2. Possible Catalytic Mechanism of Copolyester Polycondensation with Ti−M Bimetallic Coordination Catalysts
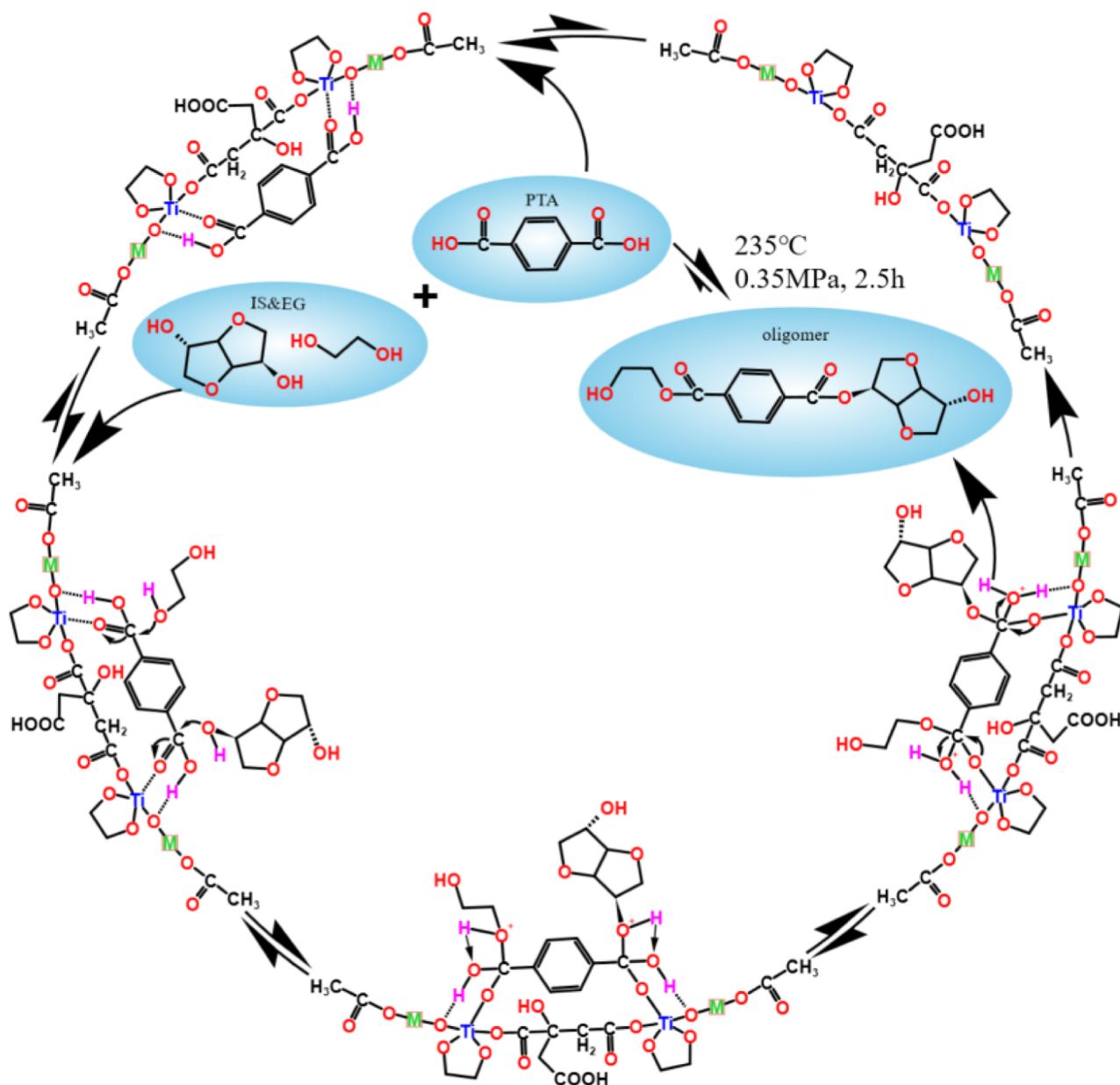

Figure 8 shows the DSC isothermal crystallization curves of the PEIT 4 catalyst at different temperatures. It can be determined from the figure that the optimal isothermal crystallization temperature of the copolyester was about 170 °C.

The crystallinity X_t of the copolyesters can be calculated by the following equation

$$X_t = \frac{\int_{t_0}^{t} \left(\frac{dH_{cryst}}{dt}\right)dt}{\int_{t_0}^{t_f} \left(\frac{dH_{cryst}}{dt}\right)dt} \tag{8}$$

where t_f is the time for complete crystallization. In addition, the relationship between X_t and the isothermal crystallization time t is presented in Figure 9a.

To further elucidate the effect of catalysts on the crystallization performance of copolyesters, we calculated the semicrystallization time $t_{1/2}$, Avrami index n, and crystallization rate constant K by the Avrami equation

$$1 - X_t = \exp(-Kt^n) \tag{9}$$

$$\log[-\ln(1 - X_t)] = \log K + n \log t \tag{10}$$

Figure 9b presents the relationship between $\lg[-\ln(1 - X_t)]$ and $\lg t$. It seems that a good linear relationship can be obtained in the early stages of crystallization for all samples except for a little deviation for PEIT 2. The upward deviation in the final stage of crystallization was mainly due to the impingement and the nonlinear growth model of the secondary crystallization.

The values of half-crystallization time$(t_{1/2})$, K, and n are listed in Table 4. It can be seen that the $t_{1/2}$ of PEIT 4, PEIT 5, and PEIT 8 is less than 15 min at 170 °C, and the semicrystallization time of PEIT 8 is as low as 10.28 min. Noticeably, the use of different catalysts has no obvious influence on the parameter n, which is always in the range of 2−3. This indicated that the catalyst has a weak effect on the crystal structure of the copolyester. The value of n of PEIT 2 is less than 2 due to the large difference between the early and late crystallization rates,

which makes the fitted line deviate too much from the data, leading to a lower value of parameter n.

3.6. Mechanical Properties of PEIT. The mechanical properties of PEIT copolyesters prepared by different catalysts are shown in Figure 10. The maximum tensile stress for copolyesters prepared by different catalysts presents approximatively, while the elongation at break demonstrates a remarkable difference. The elongation at break of PEIT 5 is the highest and reaches 33.44%, while the copolyester with the highest tensile stress was PEIT 6, which reaches 58.54 MPa. The difference in mechanical properties between the copolyesters prepared by different catalysts was caused by the ratio of isosorbide in the polymer chain and its crystallization rate when making splines. Higher molecular weight and smaller PDI make the interaction between molecular chains stronger, so that PEIT prepared by the Ti−M catalyst has a longer fracture growth rate.

3.7. Possible Catalytic Mechanism of Ti−M Bimetallic Catalysts in Copolymerization. With a combination of the chemical structure characterization and the polymerization mechanism of PET described in public work,[23,38,40,48] the possible catalytic mechanism of copolyester polycondensation with Ti−M bimetallic coordination catalysts could be speculated as Scheme 2. Compared with titanium alkoxides, titanates had higher stability, which was more conducive to the catalytic effect of catalysts under polycondensation conditions. In addition to its catalytic effect, the addition of the second metal can also increase the electron cloud density of Ti 2p through the M−O−Ti bond bridge, thereby improving the catalytic activity of titanium atoms. However, due to the autocatalytic effects and electronegativity differences of different metals, their effects on titanium atoms were not the same. As shown in Scheme 2, the carbonyl group in the carboxyl group of TPA was coordinated with Ti in the catalyst, and the hydrogen and oxygen were coordinated. Then, the diol performs a nucleophilic attack to form an intermediate, and finally, water molecules were removed to complete the reaction, and the catalyst was regenerated at the same time.

4. CONCLUSIONS

A series of new bimetallic coordination catalysts with Ti and several inexpensive and environmentally friendly transition metals were synthesized by using citric acid as a ligand, which was used in the polycondensation of the copolyester containing 10% isosorbide as a third monomer to compare with traditional monometallic antimony-based and titanium-based catalysts. The catalyst structure and activities were characterized and analyzed. FT-IR and XPS analyses indicated that the coordination reaction took place between the ligand and metal compounds in the preparation of catalysts, and the catalytic activity sequence of five bimetallic coordination catalysts characterized by DSC analysis is Ti−Zn > Sb$_2$O$_3$ > Ti−Mg > Ti−Al > Ti−Fe > Ti−Cu. The PEIT copolyesters were successfully synthesized by direct esterification−polycondensation using the bimetallic coordination catalyst with TPA, glycol, and isosorbide, and the structure, thermal properties, isothermal crystallization kinetics, and mechanical properties of PEIT were discussed. Results of the nuclear magnetic analysis of PEIT copolyesters showed that the Ti−Al bimetallic coordination catalyst demonstrated the highest reaction activity for isosorbide among the five catalysts. PEIT prepared by three catalysts Ti−Al, Ti−Mg, and Ti−Cu had higher viscosity and molecular weight, which was due to the combined effect of the difference in the catalytic activity of the second metal and the inhibition of the

activity of the titanium atom. In addition, PEIT prepared by Ti−Al showed higher T_g and T_c because of more isosorbide units in the polymer chain. As to the crystallization properties of PEIT copolyesters, the difference was attributed to the number and distribution of isosorbide units in the polymer chain derived from the different activity of catalysts. The mechanical property measurement of PEIT with different catalysts indicated that the maximum tensile stress presented approximatively, while the elongation at break of PEIT with Ti−M bimetallic catalysts generally displayed a higher value than that of either Sb-based or single metallic Ti-based catalysts.

■ AUTHOR INFORMATION

Corresponding Author

Shichang Chen − *School of Materials and Engineering, Zhejiang Sci-Tech University, Hangzhou 310018, P. R. China; Zhejiang Provincial Innovation Center of Advanced Textile Technology, Shaoxing 312000, China;* ⓞ orcid.org/0000-0002-3974-6913; Email: scchen@zstu.edu.cn

Authors

Shangdong Xie − *School of Materials and Engineering, Zhejiang Sci-Tech University, Hangzhou 310018, P. R. China*

Sitian Qian − *School of Materials and Engineering, Zhejiang Sci-Tech University, Hangzhou 310018, P. R. China*

Kaiyang Zhu − *School of Materials and Engineering, Zhejiang Sci-Tech University, Hangzhou 310018, P. R. China*

Lijiang Sun − *School of Materials and Engineering, Zhejiang Sci-Tech University, Hangzhou 310018, P. R. China*

Wenxing Chen − *School of Materials and Engineering, Zhejiang Sci-Tech University, Hangzhou 310018, P. R. China; Zhejiang Provincial Innovation Center of Advanced Textile Technology, Shaoxing 312000, China;* ⓞ orcid.org/0000-0002-4554-1455

Complete contact information is available at:
https://pubs.acs.org/10.1021/acsomega.2c07831

Notes

The authors declare no competing financial interest.

■ REFERENCES

(1) Girard, M.; Combeaud, C.; Billon, N. Effects of annealing prior to stretching on strain induced crystallization of polyethylene terephthalate. *Polymer* **2021**, *230*, 124078.

(2) Chen, S.; Chen, S.; Guang, S.; Zhang, X.; Chen, W. Film reaction kinetics for melt postpolycondensation of poly (ethylene terephthalate). *J. Appl. Polym. Sci.* **2020**, *137*, 48988.

(3) Kawai, F.; Kawabata, T.; Oda, M. Current knowledge on enzymatic PET degradation and its possible application to waste stream management and other fields. *Appl. Microbiol. Biotechnol.* **2019**, *103*, 4253−4268.

(4) Rorrer, N. A.; Nicholson, S.; Carpenter, A.; Biddy, M. J.; Grundl, N. J.; Beckham, G. T. Combining reclaimed pet with bio-based monomers enables plastics upcycling. *Joule* **2019**, *3*, 1006−1027.

(5) Ma, J.; Yu, L.; Chen, S.; Chen, W.; Wang, Y.; Guang, S.; Zhang, X.; Lu, W.; Wang, Y.; Bao, J. Structure−property evolution of poly (ethylene terephthalate) fibers in industrialized process under complex

coupling of stress and temperature field. *Macromolecules* **2019**, *52*, 565−574.

(6) Yang, Q.; Ulbricht, M. Cylindrical membrane pores with well-defined grafted linear and comblike glycopolymer layers for lectin binding. *Macromolecules* **2011**, *44*, 1303−1310.

(7) Incarnato, L.; Scarfato, P.; Di Maio, L.; Acierno, D. Structure and rheology of recycled PET modified by reactive extrusion. *Polymer* **2000**, *41*, 6825−6831.

(8) Bang, H. J.; Kim, H. Y.; Jin, F. L.; Park, S. J. Fibers spun from 1,4-cyclohexanedimethanol-modified polyethylene terephthalate resin. *J. Ind. Eng. Chem.* **2011**, *17*, 805−810.

(9) He, X.; Zhou, X.; Jia, K.; Zhang, D.; Shou, H.; Liu, X. Incorporation of polyethylene glycol into polyethylene terephthalate towards blue emitting co-polyester. *Mater. Lett.* **2016**, *182*, 367−371.

(10) Wang, L.; Wang, Y.; Zhang, F.; Bai, Y.; Ding, L. Syntheses and properties of the PET-co-PEA copolyester. *J. Appl. Polym. Sci.* **2017**, *134*, 44967.

(11) Saxon, D. J.; Luke, A. M.; Sajjad, H.; Tolman, W.; Reineke, T. Next-generation polymers: Isosorbide as a renewable alternative. *Prog. Polym. Sci.* **2020**, *101*, 101196.

(12) Weinland, D. H.; van Putten, R. J.; Gruter, G. J. M. Evaluating the commercial application potential of polyesters with 1,4:3,6-dianhydrohexitols (isosorbide, isomannide and isoide) by reviewing the synthetic challenges in step growth polymerization. *Eur. Polym. J.* **2022**, *164*, 110964.

(13) Brandi, F.; Al-Naji, M. Sustainable sorbitol dehydration to isosorbide using solid acid catalysts: transition from batch reactor to continuous flow system. *ChemSusChem* **2022**, *15*, No. e202102525.

(14) Wang, Y.; Davey, C. J. E.; van der Maas, K.; van Putten, R. J.; Tietema, A.; Parsons, J. R.; Gruter, G. J. M. Biodegradability of novel high T_g poly(isosorbide-co-1,6-hexanediol) oxalate polyester in soil and marine environments. *Sci. Total Environ.* **2022**, *815*, 152781.

(15) Park, H. S.; Gong, M. S.; Knowles, J. C. Catalyst-free synthesis of high elongation degradable polyurethanes containing varying ratios of isosorbide and polycaprolactone: physical properties and biocompatibility. *J. Mater. Sci.: Mater. Med.* **2013**, *24*, 281−294.

(16) Wilbon, P. A.; Swartz, J. L.; Meltzer, N. R.; Brutman, J. P.; Hillmyer, M. A.; Wissinger, J. E. Degradable thermosets derived from an isosorbide/succinic anhydride monomer and glycerol. *ACS Sustainable Chem. Eng.* **2017**, *5*, 9185−9190.

(17) Adjaoud, A.; Puchot, L.; Verge, P. High-T_g and degradable isosorbide-based polybenzoxazine vitrimer. *ACS Sustainable Chem. Eng.* **2022**, *10*, 594−602.

(18) Qu, D.; Zhang, F.; Gao, H.; Wang, Q.; Bai, Y.; Liu, H. Studies on isosorbide-enhanced biodegradable poly(ethylene succinate). *Chem. Res. Chin. Univ.* **2019**, *35*, 345−352.

(19) Chen, J.; Wu, J.; Qi, J.; Wang, H. Systematic study of thermal and (bio)degradable properties of semiaromatic copolyesters based on naturally occurring isosorbide. *ACS Sustainable Chem. Eng.* **2019**, *7*, 1061−1071.

(20) Japu, C.; Martínez de Ilarduya, A.; Alla, A.; Garcia-Martin, M. G.; Galbis, J. A.; Munoz-Guerra, S. D-Glucose-derived PET copolyesters with enhanced T_g. *Polym. Chem.* **2013**, *4*, 3524−3536.

(21) Gohil, R. M. Properties and strain hardening character of polyethylene terephthalate containing isosorbide. *Polym. Eng. Sci.* **2009**, *49*, 544−553.

(22) Park, S.; Thanakkasaranee, S.; Shin, H.; Ahn, K.; Sadeghi, K.; Lee, Y.; Tak, G.; Seo, J. Preparation and characterization of heat-resistant pet/bio-based polyester blends for hot-filled bottles. *Polym. Test.* **2020**, *91*, 106823.

(23) Li, X.; Song, G.; Huang, M.; Ohara, T.; Yamada, H.; Umeyama, T.; Higashino, T.; Imahori, H. Cleaner synthesis and systematical characterization of sustainable poly(isosorbide-co-ethylene terephthalate) by environ-benign and highly active catalysts. *J. Cleaner Prod.* **2019**, *206*, 483−497.

(24) Sablong, R.; Duchateau, R.; Koning, C. E.; de Wit, G.; van Es, D.; Koelewijn, R.; van Haveren, J. Incorporation of isosorbide into poly(butylene terephthalate) via solid-state polymerization. *Biomacromolecules* **2008**, *9*, 3090−3097.

(25) Wang, W.; Wu, F.; Lu, H.; Li, X.; Yang, X.; Tu, Y. A cascade polymerization method for the property modification of poly(butylene terephthalate) by the incorporation of isosorbide. *ACS Appl. Polym. Mater.* **2019**, *1*, 2313−2321.

(26) Phan, D.-N.; Lee, H.; Choi, D.; Kang, C.-Y.; Im, S. S.; Kim, I. S. Fabrication of two polyester nanofiber types containing the biobased monomer isosorbide: poly (ethylene glycol 1,4-cyclohexane dimethylene isosorbide terephthalate) and poly (1,4-cyclohexane dimethylene isosorbide terephthalate). *Nanomaterials* **2018**, *8*, 56.

(27) Marin, R.; Alla, A.; Martínez de Ilarduya, A.; Munoz-Guerra, S. Carbohydrate-based polyurethanes: a comparative study of polymers made from isosorbide and 1,4-butanediol. *J. Appl. Polym. Sci.* **2011**, *123*, 986−994.

(28) Legrand, S.; Jacquel, N.; Amedro, H.; Saint-Loup, R.; Pascault, J. P.; Rousseau, A.; Fenouillot, F. Synthesis and properties of poly(1,4-cyclohexanedimethylene-co-isosorbide terephthalate), a biobased copolyester with high performances. *Eur. Polym. J.* **2019**, *115*, 22−29.

(29) Legrand, S.; Jacquel, N.; Amedro, H.; Saint-Loup, R.; Colella, M.; Pascault, J. P.; Fenouillot, F.; Rousseau, A. Isosorbide and tricyclodecanedimethanol for the synthesis of amorphous and high T_g partially biobased copolyesters. *ACS Sustainable Chem. Eng.* **2020**, *8*, 15199−15208.

(30) Kricheldorf, H. R.; Behnken, G.; Sell, M. Influence of isosorbide on glass-transition temperature and crystallinity of poly(butylene terephthalate). *J. Macromol. Sci., Part A: Pure Appl.Chem.* **2007**, *44*, 679−684.

(31) Bersot, J. C.; Jacquel, N.; Saint-Loup, R.; Fuertes, P.; Rousseau, A.; Pascault, J. P.; Spitz, R.; Fenouillot, F.; Monteil, V. Efficiency increase of poly(ethylene terephthalate-co-isosorbide terephthalate) synthesis using bimetallic catalytic systems. *Macromol. Chem. Phys.* **2011**, *212*, 2114−2120.

(32) Stanley, N.; Chenal, T.; Delaunay, T.; Saint-Loup, R.; Jacquel, N.; Zinck, P. Bimetallic catalytic systems based on Sb, Ge and Ti for the synthesis of poly(ethylene terephthalate-co-isosorbide terephthalate). *Polymers* **2017**, *9*, 590.

(33) Wang, S.; Wang, C.; Wang, H.; Chen, X.; Wang, S. Sodium titanium tris(glycolate) as a catalyst for the chemical recycling of poly(ethylene terephthalate) via glycolysis and repolycondensation. *Polym. Degrad. Stab.* **2015**, *114*, 105−114.

(34) Massa, A.; Scettri, A.; Contessa, S.; Bugatti, V.; Concilio, S.; Iannelli, P. New catalyst for the synthesis of poly(butylene terephthalate) with high thermo-oxidative stability. *J. Appl. Polym. Sci.* **2007**, *104*, 3071−3076.

(35) Shigemoto, I.; Kawakami, T.; Okumura, M. A quantum chemical study on polymerization catalysts for polyesters: Catalytic performance of chelated complexes of titanium. *Polymer* **2013**, *54*, 3297−3305.

(36) Yang, J.; Xia, Z.; Kong, F.; Ma, X. The effect of metal catalyst on the discoloration of poly(ethylene terephthalate) in thermo-oxidative degradation. *Polym. Degrad. Stab.* **2010**, *95*, 53−58.

(37) Le Roux, E. Recent advances on tailor-made titanium catalysts for biopolymer synthesis. *Coord. Chem. Rev.* **2016**, *306*, 65−85.

(38) Li, X.; Song, G.; Huang, M. Cost-effective sustainable synthesis of high-performance high-molecular-weight poly(trimethylene terephthalate) by eco-friendly and highly active Ti/Mg catalysts. *ACS Sustainable Chem. Eng.* **2017**, *5*, 2181−2195.

(39) Liu, M.; Liu, X.; Chen, S.; Lu, W.; Li, N.; Chen, W. Determination of Molecular Weight and Distribution of Polyester by Combination of Ultra High Performance Polymer Chromatography and Laser Light Scattering. *J. Text. Res.* **2016**, *37*, 11.

(40) Li, X.; Song, G.; Huang, M.; Xie, Y. Scalable Synthesis of Poly(ester-co-ether) Elastomers via Direct Catalytic Esterification of Terephthalic Acid with Highly Active Zr−Mg Catalyst. *ACS Sustainable Chem. Eng.* **2018**, *6*, 9074−9085.

(41) Lin, Q.; Gao, F.; Wang, Y.; Lu, W.; Chen, W. Ethylene glycol-soluble Ti/Mg-citrate complex catalyst for synthesis of high intrinsic viscosity poly (ethylene terephthalate). *Polymer* **2022**, *246*, 124741.

(42) Sahu, P.; Eniyarppu, S.; Ahmed, M.; Sharma, D.; Sakthivel, A. Cerium ion-exchanged layered MCM-22: preparation, characterization

and its application for esterification of fatty acids. *J. Porous Mater.* **2018**, *25*, 999−1005.

(43) Cheng, D.; Chong, M.; Chen, F.; Zhan, X. XPS characterization of CeO2 catalyst for hydrogenation of benzoic acid to benzaldehyde. *Catal. Lett.* **2008**, *120*, 82−85.

(44) El-Toufaili, F. A.; Wiegner, J. P.; Feix, G.; Reichert, K. H. Optimization of simultaneous thermal analysis for fast screening of polycondensation catalysts. *Thermochim. Acta* **2005**, *432*, 99−105.

(45) Warren, F. J.; Gidley, M. J.; Flanagan, B. M. Infrared spectroscopy as a tool to characterise starch ordered structure-a joint FTIR-ATR, NMR, XRD and DSC study. *Carbohydr. Polym.* **2016**, *139*, 35−42.

(46) Ristic, I. S.; Vukic, N.; Cakic, S.; Simendic, V.; Ristic, O.; Budinski-Simendic, J. Synthesis and characterisation of polyester based on isosorbide and butanedioic acid. *J. Polym. Environ.* **2012**, *20*, 519−527.

(47) Descamps, N.; Fernandez, F.; Heijboer, P.; Saint-Loup, R.; Jacquel, N. Isothermal crystallization kinetics of poly(ethylene terephthalate) copolymerized with various amounts of isosorbide. *Appl. Sci.* **2020**, *10*, 1046.

(48) Scheirs, J.; Long, T. E. *Modern Polyesters: Chemistry and Technology of Polyesters and Copolyesters*; John Wiley & Sons, 2003.

■ NOTE ADDED AFTER ASAP PUBLICATION

Due to a production error, data was missing in the horizontal axis numbers of Figures 1, 2c, 3a, 4b, and 6a of the originally published version of this article. The corrected figures published May 24, 2023.